



ELSEVIER

Cold Regions Science and Technology 35 (2002) 169–184

cold regions
science
and technology

www.elsevier.com/locate/coldregions

A physical SNOWPACK model for the Swiss avalanche warning Part III: meteorological forcing, thin layer formation and evaluation

Michael Lehning^{a,*}, Perry Bartelt^a, Bob Brown^{a,b}, Charles Fierz^a

^aWSL, Swiss Federal Institute for Snow and Avalanche Research, SLF, Flüelastrasse 11, CH-7260 Davos Dorf, Switzerland

^bDepartment of Civil Engineering, Montana State University, Bozeman, USA

Abstract

The development of the seasonal snow cover is entirely driven by atmospheric forcing. SNOWPACK uses measured snow depths to determine snow precipitation rates via the calculated settling rates. This requires a rigid data control algorithm. A new statistical model is used to estimate fresh snow density as a function of the measured atmospheric conditions. A statistical model is also derived for the snow albedo, which is necessary to determine the absorbed radiation. The surface sensible and latent heat flux parameterizations are derived from Monin–Obukhov similarity and include a formulation for wind pumping. The formulations will also adapt to drifting snow conditions. The new suggestion is consistent with the observation of different roughness lengths for scalars and momentum over snow. An accurate formulation, especially for the latent heat exchange, is crucial because latent heat exchange determines the formation of surface hoar, a very important weak layer. We also account for the effect of wind pumping on the thermal conductivity in the uppermost snow layers. The surface energy and mass exchange formulations are evaluated by looking at the formation of the important thin layers surface hoar and melt–freeze crusts in SNOWPACK. Those layers are well simulated. In addition, the complete snow profile development is modeled successfully for the parameters grain type, temperature, density, grain size and liquid water content. An overall score between 0 and 1 is used to describe the profile agreement with observations and an average score of over 0.8 is reached.

© 2002 Elsevier Science B.V. All rights reserved.

Keywords: Turbulent fluxes; Surface exchange; Critical layer; Ventilation; Surface hoar

1. Introduction

In the series of three companion papers, we present the main features of the SNOWPACK model and selected evaluation results. A general introduction to SNOWPACK and snow cover modeling is given in the companion paper, Part I (Bartelt and Lehning, this

issue), and a summarizing overview is Lehning et al. (1999). The snow microstructure is described in the companion paper, Part II (Lehning et al., this issue). Here, we present the formulations that govern surface energy and mass exchange. In the evaluation part, we focus on the thin layers surface hoar and melt–freeze crusts since those two layers are dominated by the atmospheric forcing and are important layers for the avalanche warning application of SNOWPACK. In addition, we use a statistical model evaluation algorithm to give an overall assessment of the model performance.

* Corresponding author. Tel.: +41-81-417-0158; fax: +41-81-417-0110.

E-mail address: lehning@slf.ch (M. Lehning).

The development of the seasonal snow cover is almost entirely determined by the upper boundary condition, namely, the atmospheric forcing. The quality of a snow cover simulation depends, therefore, on the choice and availability of input quantities and the models used to describe surface energy and mass exchange. The formulation of adequate surface exchange parameterizations for atmospheric models has been studied extensively (Högström, 1995; Hasager and Jensen, 1999). Less work has been done on parameterizations suitable to drive snow cover models. Some particularities of the turbulent fluxes over snow and ice have been summarized by Morris (1989). The French model CROCUS is, in its operational application, driven by an artificial meteorological environment (Durand et al., 1993) and Martin and Léjeune (1998) pointed out that surface fluxes over snow and under stable conditions are higher than predicted by similarity theory. The purpose of this paper is to present a complete description of the mass and energy exchange between the snow cover and the atmosphere suitable for alpine conditions. We start with a description of the necessary input data to run SNOWPACK and point to the importance of data control routines for an automatic model operation. As a second step, the models of the surface mass and energy exchange are presented. Processes modeled are snowfall, rain, shortwave and longwave radiation, sensible and latent (surface hoar formation, sublimation) heat exchange and wind pumping. Also included is snow drift, which has already been presented in Lehning et al. (2000). Some of the formulations used are already known and we only list them with the appropriate reference. Other formulations are new or adapted and we present them in more detail. It is beyond the scope of the current paper to give an exhaustive evaluation of all the single model components. Where such a specific evaluation has already been done or is currently undertaken, it is mentioned or referenced.

2. SNOWPACK input parameters and surface mass and energy exchange

SNOWPACK requires the following input parameters: the air temperature, the relative humidity and the wind speed. Since the albedo is calculated by a sta-

istical model, reflected or incoming shortwave radiation can be provided. According to the choice of boundary condition, incoming longwave radiation (or atmospheric emissivity) and/or snow surface temperature can be provided. If both are provided, the model uses snow surface temperature as long as it is well below melting temperature (-1.3 °C). In case neither snow surface temperature nor incoming longwave or atmospheric emissivity can be obtained, SNOWPACK estimates the atmospheric emissivity and calculates the incoming longwave radiation. In addition, the interface temperature at the ground should be known and is assumed to be at the melting temperature otherwise. SNOWPACK requires further the measured snow height or the new snow water equivalent (rain rate) to determine the mass added through snowfall.

These input parameters can be provided as a simple ASCII file. In our operational application, they are read from a data base. In the near future, SNOWPACK will also be driven by the output from the operational Swiss meteorological forecast model.

2.1. IMIS stations and data control

In the Summer of 1996, the Swiss Federal Institute for Snow and Avalanche Research (SLF) started to set up a network of high Alpine automatic weather and snow stations (IMIS)¹ in cooperation with the Swiss mountain cantons (Lehning et al., 1999). An automatic IMIS station consists of a wind station situated on top of a mountain peak and a snow station close to the wind station but on a rather flat site with a limited influence of snowdrift. The snow stations are located at altitudes of typical avalanche starting zones, i.e. between 1600 and 3000 m a.s.l. Measured parameters are wind, air temperature, relative humidity, snow depth, surface temperature, soil temperature, reflected shortwave radiation and three temperatures within the snow cover. The stations operate autonomously using a battery and a solar panel. Therefore, the sensors can not be heated or ventilated. Some measurement errors and data gaps occur because of this limitation. Experience gathered during the last four winters shows, however, that the operation of the stations remains stable and reliable for most of the winter season. On all of the approximately

¹ German: Interkantonaies Mess-und Informations-System.

80 snow stations in operation during the winter of 2000/2001, the model is operationally run and provides information on the snow cover.

Because of the occasional measurement errors and gaps, it is necessary to control and correct erroneous data before using the data as input for the snowpack model calculation. All measured input parameters need to be within reasonable physical limits. In addition, all measured time series are checked for outliers based upon a Huber type skipped mean, which uses the median absolute deviation (Hampel, 1985). Gaps are filled by a linear interpolation.

The snow height measurements with an ultrasonic sensor require special treatment because they determine the amount of new snow and are at the same time particularly prone to measurement errors and typically produce a noisy signal. We, therefore, have formulated a control procedure which eliminates spikes from the time series, checks for outliers and physical limits and uses maximum changes in snow depth. Details on the snow depth control routine are found in Appendix A. Our heuristic data control routine has been found to guarantee a stable automatic operation of SNOWPACK at more than 80 IMIS stations.

2.2. Treatment of new snow and determination of precipitation rates

The IMIS stations do not measure precipitation and it is well known that snow precipitation measurements are not very reliable. In addition, meteorological model predictions for alpine terrain are not very reliable. Therefore, we use an alternative method to determine snow precipitation as input for our snowpack model calculations. Provided that the model calculates a correct settling rate and that the corrected snow depth measurement is free of errors, the amount of new snow can be obtained by the following procedure. For every time step, the expected model snow depth, hs^{model} , without new snow precipitation is calculated and compared to the measured snow depth, hs^{valid} . The new snow height for this time step, hns , is then simply taken as the difference:

$$hns = hs^{\text{valid}} - hs^{\text{model}} \quad (1)$$

This procedure neglects the additional settling introduced through the new snow weight during the

time step in which the new snow falls. With our numerical time discretization of 15 min, the error is small. We note that currently negative deviations, i.e. model underestimation of settling rates, are not accounted for and are a potential problem. Possible erosion by wind is accounted for and is described in detail in Lehning et al. (2000). The evaluation in Section 3 shows that we do predict reliable settling rates.

The amount of new snow, hns , is added to the model as new elements. As a further check, this is only done if relative humidity is higher than 70% and reflected shortwave radiation is lower than 250 W m^{-2} . It is obvious that this procedure adapts the model snow height to the measured snow height during periods of snowfall. A crucial part of the outlined procedure with respect to a correct total mass balance is, therefore, the estimation of the initial new snow density. The new snow density, ρ , are estimated using the following relationship statistically derived from measurements at Davos, Flüelastrasse (1560 m a.s.l.) at Parsenn Kreuzweg (2290 m a.s.l.) and at the experimental site Weissfluhjoch (2550 m a.s.l.):

$$\rho = \alpha + \beta TA + \gamma TSS + \delta RH + \eta VW + \phi TA \text{ TSS} \\ + \mu TA \text{ VW} + \nu RH \text{ VW} + \sigma TA \text{ TSS} \text{ RH} \quad (2)$$

Table 1 explains the variables used and the estimation of the parameters based upon a robust regression analysis. All terms are highly significant ($p < 0.001$) and an approximate multiple coefficient of determination (r^2) of 0.83 is obtained. The assumptions for a linear statistical model, such as normal distribution of the residuals, are met. The data have a limited range of the explanatory variables air temperature and surface temperature, as well as of the observed densities (Table 1). To avoid erroneous extrapolation, the density prediction is, thus, limited to a range from 30 to 150 kg m^{-3} . We emphasize that the regression is valid for a 30–60-min time interval and not for 24-h new snow.

The procedure to determine the new snow amounts allows also to estimate current snow precipitation rates, provided that the net snow transport through wind is negligible for the IMIS snow stations. The density profile evaluation in Section 3, as well as the

Table 1

Parameters for the new snow density model based on a dataset of 84 observations

Quantity	Description	Unit	Range measured
ρ	snow density	kg m ⁻³	32 to 140
TA	air temperature	°C	-12 to +2
TSS	surface temperature	°C	-12 to 0
RH	relative humidity	%	46 to 100
VW	wind speed	m s ⁻¹	0 to 12

Parameter	Value
α	70
β	6.5
γ	7.5
δ	0.26
η	13
ϕ	-4.5
μ	-0.65
ν	-0.17
ω	0.06

mass balance evaluation in Part I, show that reliable precipitation rates are obtained.

2.3. Surface heat fluxes, surface hoar and rain

The surface heat fluxes are at present parameterized assuming a neutral atmospheric surface layer and using Monin–Obukhov similarity theory. The assumption of a neutral atmospheric surface layer is justified over snow in the presence of moderate to high wind speeds in our complex terrain setting. Slightly stable conditions may be present at low wind speeds. It is important to note that the height of the measurement sensors above the snow surface changes in the course of the winter considerably. This effect is taken into account when parameterizing the surface fluxes with Monin–Obukhov similarity. Because wind pumping is an important aspect of the surface energy exchange and the heat transfer (Section 2.4), we choose a description analogous to canopy flow (Kaimal and Finnigan, 1994) and postulate that the wind speed does not vanish at the snow surface. This is a new suggestion and has the advantage that a consistent flux formulation is still possible. The vertical coordinate, z , is zero at the snow surface and we define a displacement depth, d , using the observation that for snow with a density, ρ , of 100 kg m⁻³, the effect of wind pumping vanishes typically at a depth of 0.3 m (Sokratov and Sato, 2001). With the

further assumption that snow is typically more effective in attenuating the flow than a canopy, we use as a first estimate for the displacement depth:

$$\int_{-d}^0 \rho(z) dz = 0.5 \text{ kg m}^{-2}. \quad (3)$$

In the absence of a more accurate alternative (only measurements at one height above the snow available), we then start with the logarithmic wind profile:

$$u(z) = \frac{u_*}{k} \ln \frac{z+d}{z_0}. \quad (4)$$

Using the measured wind speed, $u(z)$, and knowing the displacement height, d , we can solve for the friction velocity, u_* , and the roughness length, z_0 , iteratively as described in Lehning et al. (2000). Note that this method also includes the possible effects of drifting snow. k is the von Karman constant. From similarity theory (Stull, 1988), the gradient of the scalar quantity temperature, T , takes the form:²

$$\frac{\partial T}{\partial z} = \frac{-0.74}{kz u_*} \frac{Q_s(z)}{\rho_a c_p}. \quad (5)$$

$Q_s(z)$ is the sensible heat flux, ρ_a the density of air and c_p the heat capacity. In the absence of better knowledge, we make the simplifying assumption that the scalar surface layer profiles are still valid in the presence of wind pumping. In the surface layer (constant flux layer), the fluxes at any height are approximately equal to the surface flux, $Q_s(z) = Q_s(0)$. The surface is not entirely smooth and the roughness length, z_0 , is a parameter describing the aerodynamic surface roughness. It is also known that the roughness length is always smaller than the height of the individual roughness elements (Stull, 1988). Thus, the measured surface temperature is postulated to be the temperature at z_0 : $T(z_0) = T(0)$. We can now integrate Eq. (5) from z_0 to the height of the measured air temperature to receive:

$$T(z) - T(0) = \frac{-0.74}{k u_*} \frac{Q_s(z)}{\rho_a c_p} \ln \frac{z}{z_0}. \quad (6)$$

² Note here that since we are only concerned with minor changes in altitude within the surface layer, we do not have to use potential temperature instead of temperature.

and the surface sensible heat flux, $Q_s(0)$ can be obtained from the measurement of wind speed and temperature at any height, z , and the surface temperature, $T(0)$:

$$Q_s(0) = \frac{-ku_*}{0.74 \ln \frac{z}{z_0}} \rho_a c_p (T(z) - T(0)). \quad (7)$$

Note that no displacement depth is considered for the scalar profiles. This has the desired effect that the observed differences between the aerodynamic roughness length, z_0 , and the corresponding roughness lengths for scalars especially over (melting) snow (Calanca, 2001) is accounted for in our formulation. However, more basic research is clearly needed to test this hypothesis. It is also easily seen that Eq. (7) is analogous to the form of the usual bulk transfer equation for surface fluxes and suggests an expected value for the kinematic transfer coefficient, C :

$$C = \frac{ku_*}{0.74 \ln \frac{z}{z_0}}. \quad (8)$$

The development for the latent heat flux, Q_l , is identical and we receive using (Eq. (8)):

$$\begin{aligned} Q_l &= -C \frac{0.622L^{w/i}}{R_a T(z)} [e_s^w(T(z))rH - e_s^i(T(0))] \\ &= -C \frac{0.622L^{w/i} \rho_a}{p_a} [e_s^w(T(z))rH - e_s^i(T(0))]. \quad (9) \end{aligned}$$

R_a ($287 \text{ J kg}^{-1} \text{ K}^{-1}$) is the gas constant for dry air, $L^{w/i}$ ($2256/2838 \text{ kJ kg}^{-1}$) are the latent heat values for vaporization and sublimation, respectively, $e_s^{w/i}$ is the saturation vapor pressure (Pa) over water or ice and p_a is the air pressure. At the snow surface, we take the saturated vapor pressure over ice. The saturation vapor pressure is approximated by a common semiempirical relationship that uses the triple point pressure, p_t (610.5 Pa), $L^{w/i}$, the triple point temperature, T_t (273.16 K) and the water vapor gas constant, R_v ($461.9 \text{ J kg}^{-1} \text{ K}^{-1}$):

$$e_s(T) = p_t e^{\frac{L^{w/i}(T-T_t)}{R_v T_t T}}. \quad (10)$$

We choose this simple surface flux parameterization because it proved to be stable for our sometimes

inaccurate automatic measurements and because most of the time deviations from near neutral conditions are small. A more accurate formulation taking into account stability effects is in preparation and will be used for research applications.

The formation of surface hoar is an important process because surface hoar constitutes a weak layer when buried by new snow. In principle, the exchange of latent heat (Eq. (9)) also determines the amount of surface hoar formed. However, observations show that there is not a very good correlation between observed surface hoar and the cumulative latent heat exchanged during a clear night when considerable surface hoar formed. This is mainly due to the fact that surface hoar formation ceases for larger than moderate wind speeds (Hachikubo and Akitaya, 1997). Föhn (2001) has undertaken systematic quantitative measurements of surface hoar and the accompanying meteorological conditions. He found that best results with bulk transfer models of latent heat are obtained if surface hoar formation is taken as latent heat exchange with wind speeds lower than 3 m/s . Sublimation (ablation) of surface hoar is simply taken as the latent heat flux. An evaluation of this procedure is given in Section 3.2.

The energy added to the snow cover by (warm) rain, Q_r , is also treated as a flux boundary condition. We assume that rain has the same temperature as the air and, thus, the flux of energy due to rain is given by:

$$Q_r = r_r c_p (T_a - T_{SS}). \quad (11)$$

Here r_r (kg s^{-1}) is the rain rate and c_p the specific heat of water ($4190 \text{ J kg}^{-1} \text{ K}^{-1}$). The rain mass is added to the uppermost element of the snow cover and the water will then undergo phase changes or will be transported downwards (Part I). Note that in case of snow temperatures below $0 \text{ }^\circ\text{C}$ most of the effect of rain on snow will be due to the phase change energy when the water freezes.

2.4. Wind pumping

There is evidence that air flow within the upper snow layers greatly affects the heat budget, as well as vapor transport (e.g. Sokratov and Sato, 2001; Albert and McGilvary, 1992), even though there are contradictory results on the mechanism of flow generation

within the snow cover (Colbeck, 1997; Sokratov and Sato, 2000). We propose the following simplified model for our one-dimensional SNOWPACK model. We point out that a more accurate description, such as Albert and McGilvary (1992), is preferable but impossible to implement in a one-dimensional model. We already proposed a formulation of the effect of wind pumping on the wind profile above the snow cover (Eq. (4)) and, thus, on the turbulent flux parameterization and have now to find a parameterization to include the effect on the snow cover itself. The main effect is an increase in heat and vapor transport (Albert and McGilvary, 1992). In SNOWPACK, this effect is best accounted for by increasing the thermal conductivity as obtained from our microstructure model (Part II) and the water vapor diffusivity. This will then affect not only heat transport but kinetic grain and bond growth as well. We assume that the effect of wind pumping decreases exponentially from the snow cover surface and define a wind pumping velocity scale, \hat{u} :

$$\hat{u} = u(0)e^{\alpha z}, \text{ with } \alpha = 0.1 \text{ m}^3 \text{ kg}^{-1} \rho(z). \quad (12)$$

Here $u(0)$ is the surface velocity according to Eq. (4), z is negative below the snow surface and ρ (kg m^{-3}) is the snow density, which also varies with depth. Using a mixing length approach, where the length scale is the pore length, L_p , a diffusivity due to wind pumping, K_p , can be defined:

$$K_p = \beta L_p^2 \left| \frac{d\hat{u}}{dz} \right|. \quad (13)$$

The pore length is approximated by 1.6 times the grain radius (Part II). Theoretically, the coefficient, β , is the ratio of tortuosity to porosity. We use β as a fitting parameter. K_p is added to the effective thermal conductivity (Part II) with $\beta=0.02$. The current version of SNOWPACK only uses this effect on the thermal conductivity. It is expected that Eq. (13) also holds for the vapor diffusivity but more detailed experiments are required to determine the corresponding value of β .

With the effect of wind pumping on the thermal conductivity, improved simulations of the thermal regime in the snow cover are possible. As pointed out above, this only concerns the uppermost layers, however. Since superficial melting and surface hoar

formation takes place at or close to the surface, wind pumping also affects the formation of thin and dangerous layers. The effect of wind pumping on SNOWPACK simulation results is discussed in Section 3.

2.5. Radiation

2.5.1. Atmospheric emissivity and longwave radiation

In general the measured surface temperature is used as an upper boundary condition as long as it is below -1.3 °C. However, as soon as the surface temperature approaches phase change temperatures and for special (research) applications, the complete energy exchange at the upper boundary including the longwave radiation must be known. In the absence of cloud observations, we follow Brutsaert (1975), for the atmospheric emissivity, ea ,

$$ea = 1.24 \left(\frac{e_s(TA)RH}{TA} \right)^{\frac{1}{7}}. \quad (14)$$

The net longwave radiation, R_n^l , is then:

$$R_n^l = -\sigma(eaTA^4 - TSS^4). \quad (15)$$

Cloudiness is neglected at the moment. A feasible suggestion for our IMIS stations has been made by Gubler (1998). He suggested to estimate cloudiness from a comparison between potential and measured shortwave radiation. This procedure might be implemented in a later version of SNOWPACK.

2.5.2. Albedo, shortwave radiation and extinction coefficient

Since shortwave radiation dominates the energy balance of Alpine snowpacks, the formulation of the surface albedo is a very important part of a snowpack model. We chose to develop a statistical model based on continuous measurements over 3 years at the Weissfluhjoch experimental site. The measurements are made with instruments equivalent to the IMIS sensors. Thus, the model is expected to provide an optimal albedo function, A , for our measurement configuration. Here, we present two models. One is exclusively based on measured meteorological parameters, while the second model includes (modeled) snowpack parameters. The models have the form:

$$A = \alpha + \ln(1 + x). \quad (16)$$

Here, x is a linear function of the meteorological parameters:

$$x = \beta VW + \gamma TA + \delta TSS + \eta RSWR + \kappa TA \text{ TSS} + \lambda TA \text{ RSWR}, \quad (17)$$

or for the second model including SNOWPACK parameters:

$$x = \beta VW + \gamma TA + \delta TSS + \eta RSWR + \kappa TA \text{ TSS} + \lambda RHO + \mu WC + \nu RB + \omicron DN + \pi SP + \theta FR. \quad (18)$$

The model parameters and coefficients are summarized in Table 2. An arbitrary piece of a time series of measured albedo, which had not been used for the

model development, is drawn in Fig. 1, together with the two modeled albedo time series according to Eq. (16) with Eq. (17) (simple model) or with Eq. (18) (complete model), respectively. The overall agreement between modeled and measured values is very good. Deviations are visible in the high-frequency variability, which is unimportant for the overall energy balance. All variables and their combinations are highly significant ($p < 0.001$) and the statistical model fulfills the assumption of uncorrelated and normally distributed residuals. It is concluded that the statistical model is a good description for the variation of the albedo.

The measured reflected shortwave radiation, RSWR, serves to determine the input of shortwave radiation to the snow cover.³ The amount of shortwave energy absorbed by the snow cover, $R_s^a = RSWR / (A - 1)$, is treated as a body (volume) source. At the layer/element boundaries, the residual radiation is calculated, $R_s^r(l) = R_s^a e^{-k_{ext}l}$, where l (m) is the distance from the snow cover surface and k_{ext} is the extinction coefficient (m^{-1}). The amount of energy absorbed in the snow layer between $l2$ and $l1$ is then $R_s^r(l1) - R_s^r(l2)$. The extinction coefficient varies linearly with snow density:

$$k_{ext} = \frac{\rho}{c1} + c2. \quad (19)$$

The parameters are $c1 = 3 \text{ kg m}^{-2}$ and $c2 = 50 \text{ m}^{-1}$.

3. Evaluation

The following results are representative for the operational application. It is beyond the scope of this paper to evaluate all individual model components. However, we want to assess the performance of the model in representing important thin layers, such as surface hoar and melt–freeze crusts. These layers are directly influenced by atmospheric forcing as discussed in this paper. In addition the overall performance of SNOWPACK in simulating profiles of grain

Table 2
Parameters for the albedo function

Quantity	Description	Unit
VW	wind speed	$m \text{ s}^{-1}$
TA	air temperature	K
TSS	surface temperature	K
RSWR	reflected short-wave radiation	$W \text{ m}^{-2}$
RHO	snow density	$kg \text{ m}^{-3}$
WC	fractional water content	0 to “threshold”
RB	bond radius	mm
DN	dendricity	0 to 1
SP	sphericity	0 to 1
FR	categorical variable indicating previous melt and refreeze	0 or 1

Parameter	Value model (Eq. (17))	Value model (Eq. (18))
α	0.8 (mean value)	0.8 (mean value)
β	0.0053	0.0056
γ	−0.041	−0.052
δ	0.016	0.0084
η	−0.0015	− 6.8×10^{-5}
κ	− 4.2×10^{-5}	− 1.1×10^{-5}
λ	− 5.3×10^{-6}	−0.00030
μ	−	−3.0
ν	−	0.060
\omicron	−	0.017
π	−	0.021
θ	−	−0.032

³ We measure reflected shortwave radiation with a sensor that is looking down in order to minimize problems with snowfall and riming.

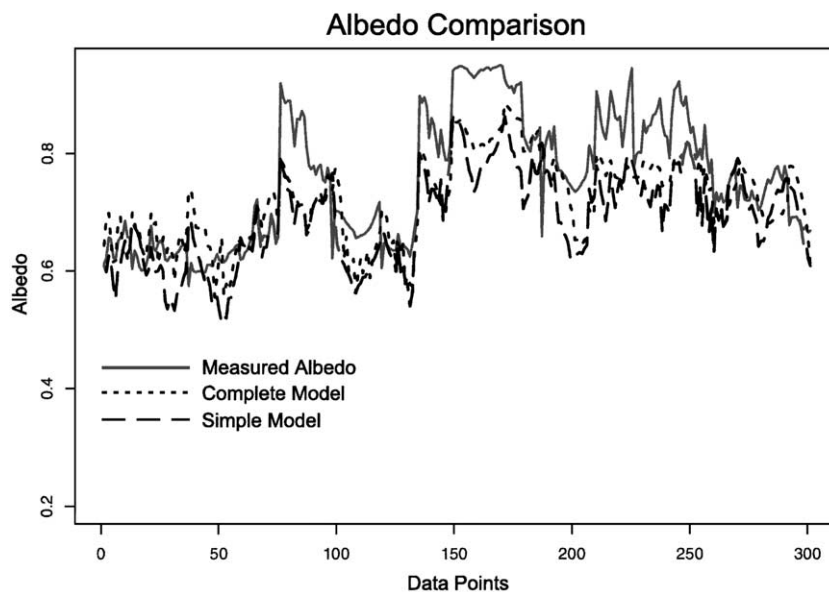


Fig. 1. Comparison between statistical albedo estimation and an independent data set.

type, temperature, density, grain size and liquid water content is evaluated using a statistical agreement score. This score allows to quantitatively monitor model improvements. Additional detailed evaluations are undertaken elsewhere. Such evaluations include a complete mass balance assessment (Part I), detailed layer by layer settling evaluation (Fierz and Lehning, 2001), the application of SNOWPACK to continental snow covers (Lundy et al., 2001) and systematic profile comparisons for different sites (Lehning et al., 2001). A description and evaluation of the drift index implemented in SNOWPACK is Lehning et al. (2000).

3.1. Qualitative evaluation of thin layer formation

SNOWPACK is not only an energy and mass balance snow model but aims at giving a detailed description of the layered structure of the snow cover. Especially critical layers for avalanche formation, such as buried surface hoar, depth hoar and crusts, need to be adequately modeled. Such thin layers are a challenge to modelers because their formation involves all the processes of surface energy exchange as discussed in this paper. Therefore, we present a case study evaluation on how SNOWPACK performs

in representing layers of surface hoar and melt–freeze crusts in the seasonal snow cover. The only reference sources of snow cover information available are snow pit profiles taken by experienced observers. We present two representative profiles, one from the winter 1997/1998 (Fig. 2) and one from the avalanche winter 1998/1999 (Fig. 3). Both profiles have been taken by an experienced avalanche expert at the Weissfluhjoch experimental site.

Fig. 2 shows the grain type development for all of the winter of 1997/1998 as simulated by SNOWPACK. The observed profile of March 2, 1998 is drawn for comparison. An excellent agreement is found for the sequence of thin layers at the top of the snow cover: The layer of fresh, dendritic snow at the top, then the first melt–freeze crust followed by a layer of near surface faceted crystals and the second melt–freeze crust are present in the observed and in the simulated profiles. Some decomposed crystals in the layer of near-surface faceted crystals have been detected by the observer, which are no longer present in the model. For the bulk of the snow cover, the observer gave a uniform layer of faceted crystals, while more variation in the degree of faceting is present in the model. The model even predicts rounded grain shapes in the center of the snow

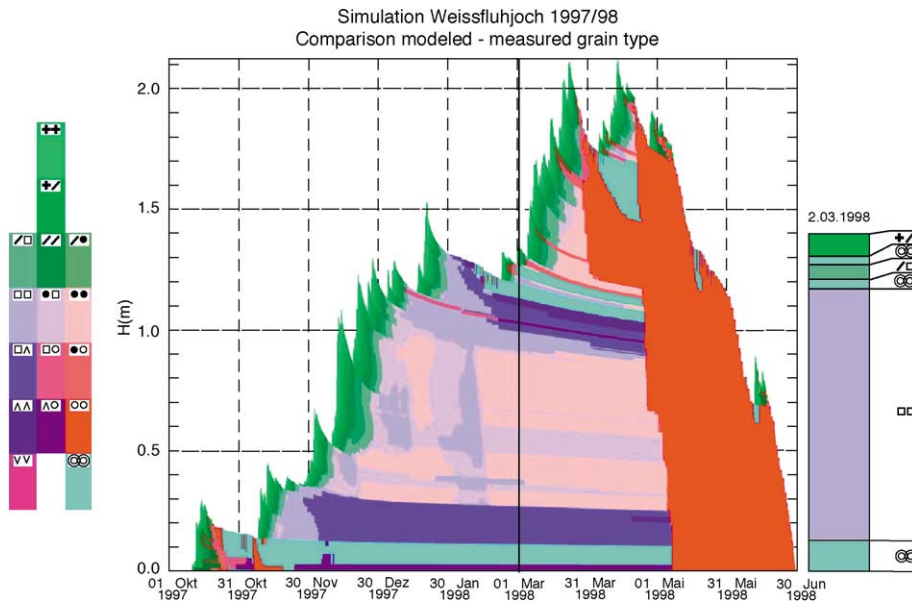


Fig. 2. SNOWPACK grain-type simulation for the entire winter 1997/98. A manually observed profile at the beginning of March is drawn for comparison. Grain types are represented by different colors. The symbols are explained in Fig. 8 of Part II. The sequence of thin layers at the surface is well captured by the model.

cover. The crust at the bottom of the snow cover is then again present in the model, as well as in the observation.

Fig. 3 is similar to Fig. 2 but only a part of the seasonal simulation is shown to allow a better representation of the layer details. Again, the comparison

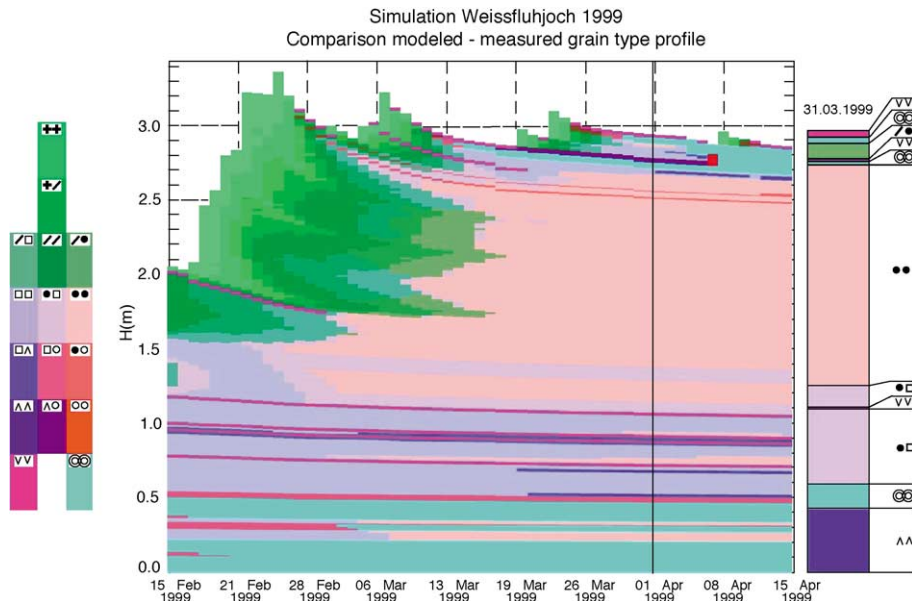


Fig. 3. SNOWPACK grain-type simulation for part of the winter 1998/1999. The manually observed profile at the end of March is drawn for comparison. All observed surface hoar layers are modeled.

between the observed profile of March 31, 1999 and the simulation shows an excellent agreement for the sequence of thin layers at the top of the snow cover: At the surface, a period of fair weather has created a surface hoar layer sitting on top of a melt–freeze crust. The snow from the two smaller snowfall events around March 23 consists of decomposed to rounded crystals according to the observation, while the simulation sees rounded to faceted crystals. The period of fair weather of mid March had again created surface hoar sitting on a crust. The simulation for these layers is almost identical to the observation. Model and simulation agree also in the deep layer of rounded crystals below the thin layers at the surface. Then, below an area with more faceting, a buried surface hoar layer is found. This dangerous layer might have played a role in some of the catastrophic avalanches in February 1999. The simulation shows this layer. The lowest part of the snow profile shows in general more faceting. The model has additional buried surface hoar layers, which have not been found by the observer. Note that a buried surface hoar layer is very difficult to see and even an experienced observer might miss such a layer. While both model and observation have another melt–freeze

crust at about 0.5 m above ground, the model simulates two additional crusts, which are not seen in the observation.

These two representative profiles suggest that SNOWPACK is able to give a very realistic picture of the layered snow cover structure. This is especially important for critical thin layers, such as surface hoar and melt–freeze crusts.

3.2. Surface hoar formation and sublimation rates

Buried surface hoar is one of the most critical factors for the stability of an Alpine snow cover. In the section above, we have demonstrated that SNOWPACK is able to predict reasonably surface hoar formation and conservation for the avalanche winter 1999. For the same winter, Föhn (2001) has collected precise and sufficient data on surface hoar formation and sublimation rates to allow a more quantitative evaluation. Fig. 4 shows a scatter plot of simulated versus observed surface hoar formation rates. Fig. 4a is for a best-fit bulk exchange coefficient (Föhn, 2001), which gives the highest coefficient of determination (r^2) of 0.89. With the adapted Monin Obukhov similarity approach used in SNOWPACK, the coefficient

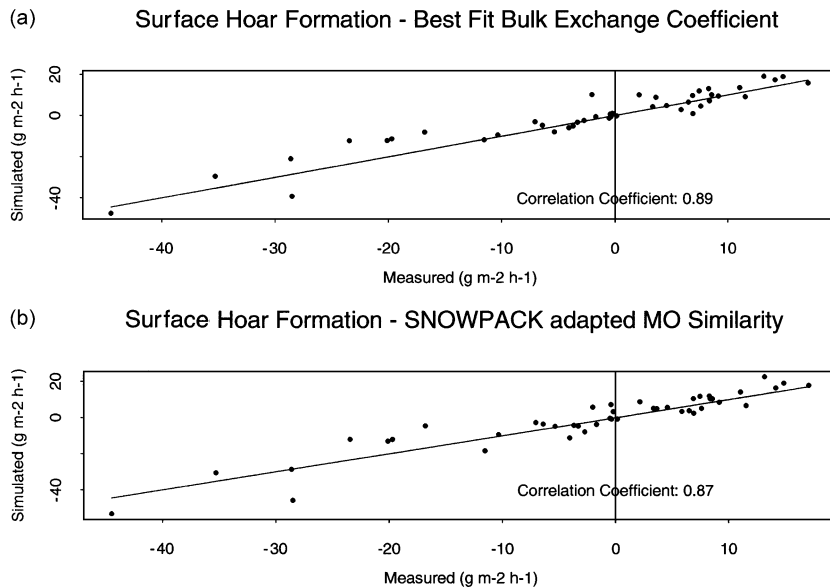
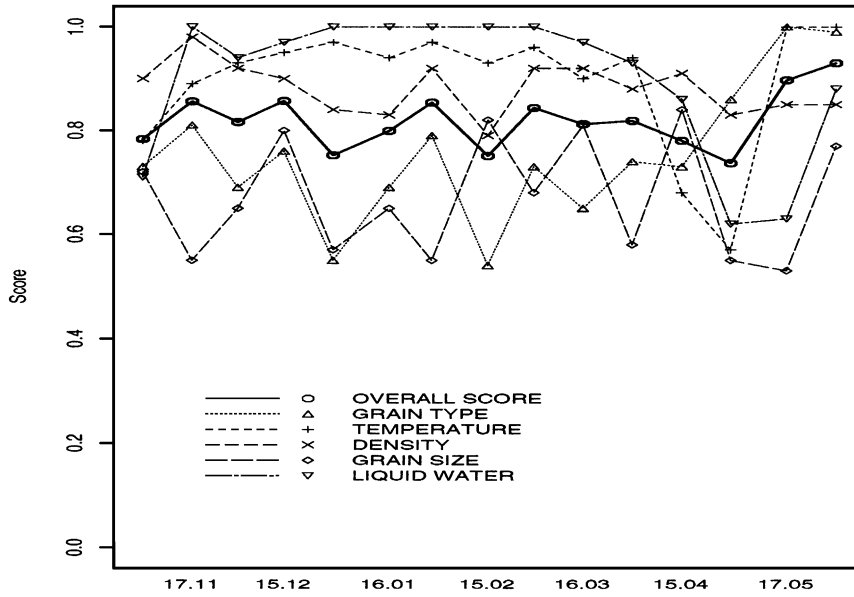


Fig. 4. Comparison of model surface hoar formation and ablation rates with observations. The results with a fitted exchange coefficient (a) are only slightly better than the results for the theoretical formulation used in SNOWPACK (b).

a Agreement Score at Weissfluhjoch Versuchsfeld 1992/93



b Agreement Score at Weissfluhjoch Versuchsfeld 1995/96

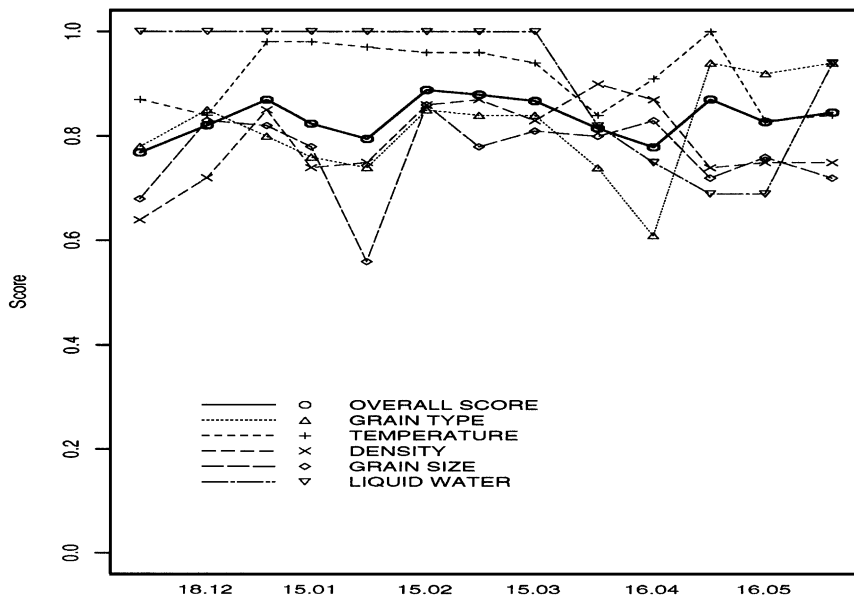
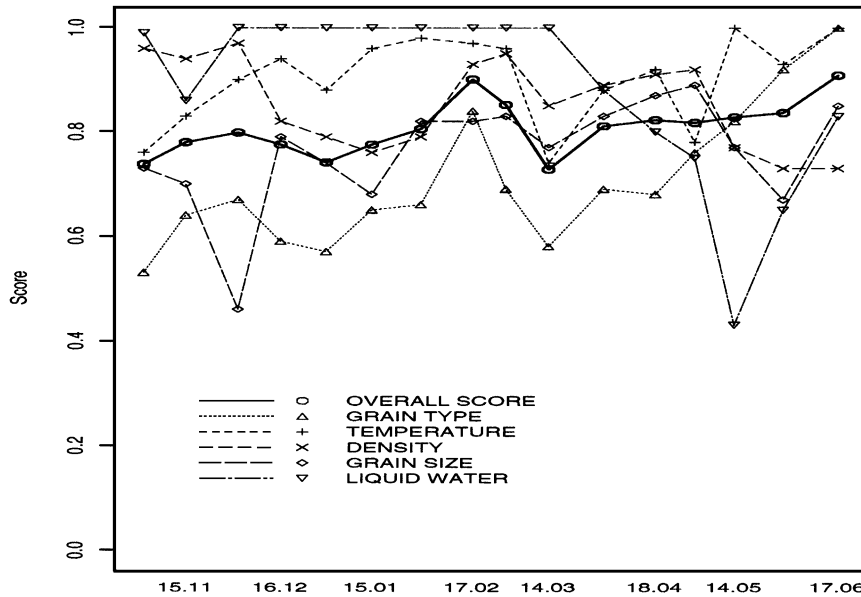


Fig. 5. Evaluation of SNOWPACK profile predictions for five complete winter seasons at the Versuchsfeld Weissfluhjoch experimental site. The evaluation is done using the objective snow profile comparison method (Lehning et al., 2001). This method gives a quantitative nondimensional agreement score between 0 and 1. Compared are manual profiles taken by snow experts and the model predictions.

of determination is only slightly lower ($r^2=0.87$; Fig. 4b). Note that the exchange coefficient in SNOWPACK is entirely determined by theoretical consider-

ations. Therefore, it can be expected that similar good results are obtained for different locations and meteorological conditions.

c Agreement Score at Weissfluhjoch Versuchsfeld 1996/97



d Agreement Score at Weissfluhjoch Versuchsfeld 1997/98

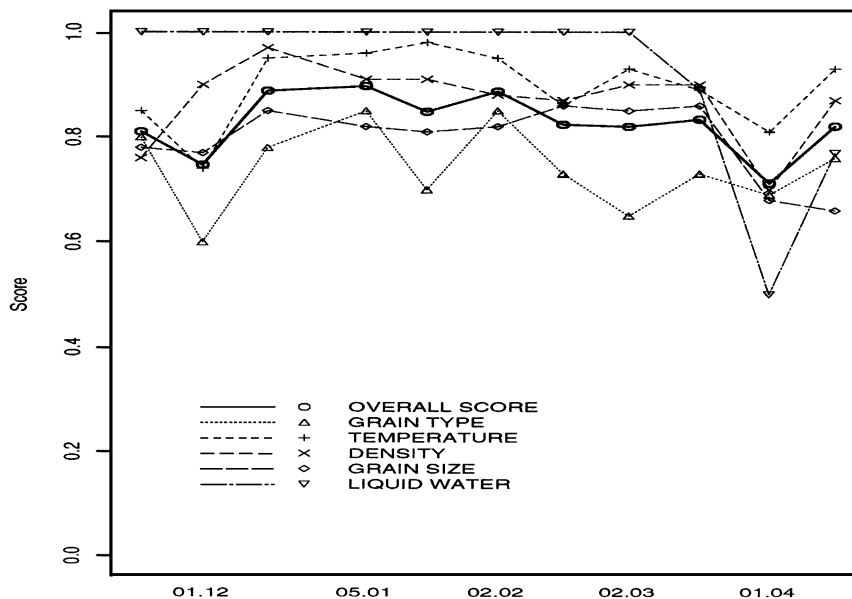


Fig. 5 (continued).

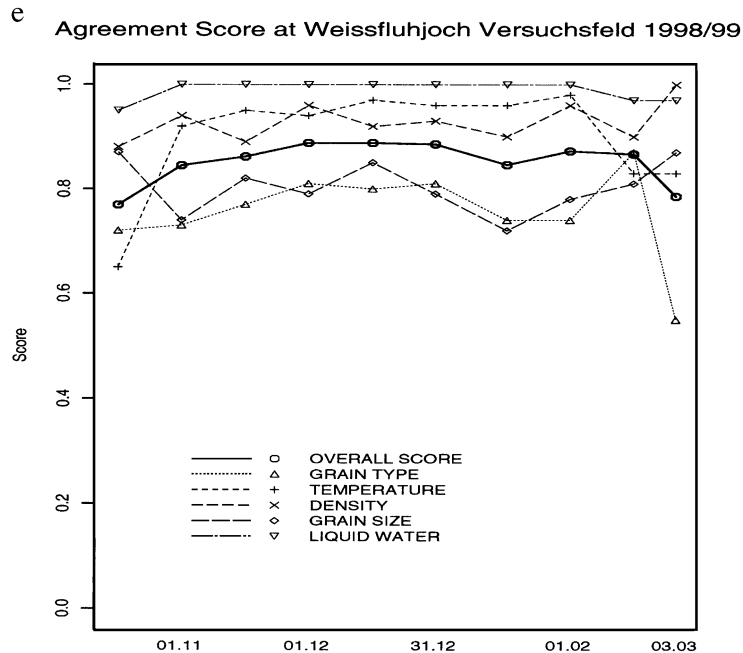


Fig. 5 (continued).

3.3. Quantitative profile comparison

In Section 3.1, we presented a qualitative comparison between simulated and observed snow profiles. In Section 3.2, an individual process, namely surface hoar formation, has been evaluated quantitatively. However, we also want to have a quantitative measure of agreement for the whole profile. A direct use of observed profiles for quantitative snow cover simulation evaluation is difficult because of the difference in parameters simulated and observed (e.g. bond size versus hand hardness) and not least because of the different formats and resolutions used. These differences arise from simulation requirements and practical constraints in the field, respectively. We, therefore, use an objective profile comparison method to assess the overall performance of the model. The comparison is made for the parameters temperature, density, snow type, snow liquid water content and grain size. A quantitative agreement–disagreement score is calculated for each parameter. The score is normalized to vary between “0” and “1.” A “1” means that the profiles are identical, e.g. that for grain type every layer from the manual profile is also present with approx-

imately the same characteristics and the same layer thickness in the model. The individual scores are finally combined to give an overall score of profile agreement. The comparison method is fully documented in Lehning et al. (2001).

Fig. 5 summarizes the individual and the overall scores for five winters, which have not been analyzed previously. The overall score is on average above 0.8 with a small intraannual scatter. It is slightly higher than for the two stations analyzed in Lehning et al. (2001) due to improvements in this newer model version, which now includes a parameterization of wind pumping (Eqs. (12) and (13)) and an improved turbulent flux parameterization (Eqs. (7) and (9)). When analyzing the individual scores, we see that systematically some quantities are better predicted. Of course, the score for liquid water has to be “1” as long as model and observed profiles are both completely dry. Consistently for all years and all parts of the winter season, temperature is predicted best, followed by density, while on average grain size and grain type show more scatter and a lower score. It is justified to conclude that the partly empirical formulations governing grain growth and metamorphism

(Part II) are less accurate than the formulations for the mass and energy balance. However, we have also to bear in mind that grain sizes and grain types are estimated by eye in those observed profiles. Some of the scatter is certainly due to variations in the observer's performance. The same constraint applies to the determination of liquid water content, which is still estimated by "hand" in the observed profiles used here. Therefore, it is hard to decide whether the marked drop in the liquid water score during the onset of melt conditions in spring is due to an insufficient water transport scheme (Part I), or due to biases in the hand measurements. There is only a small decrease in the temperature score during the same time and the onset of isothermal conditions, as well as the melt rates (Part I), are accurately predicted. Therefore, the problem appears not to be in the energy part but has to be in the water transport part, provided that the hand estimations are correct. For those years with profile measurements until early summer (Fig. 5a, b and c), it is seen that the scores for grain type, temperature, liquid water content and also grain size recover after the drop. This is to be expected since the whole snow cover is made up of melt forms, is isothermal and saturated with water in the model and in the observations during a large part of the final melting stage.

Returning to our main focus, namely, the formation of thin layers, the profile comparison method can now also be used to quantify improvements made when adding new modules to the model. For example, the parameterization of wind pumping increases the temperature agreement score for the profiles in Fig. 3 from 0.81 to 0.96.

4. Conclusions and outlook

As the third part of the full description of the snow cover model SNOWPACK, we presented the model of atmospheric forcing, we discussed thin layer formation and presented an evaluation. The overall evaluation shows that for high Alpine sites the current version of SNOWPACK is an accurate description of the development of the seasonal snow cover, given the complexity of the subject.

Since emphasis of the model is on its operational application for the avalanche warning services in Switzerland, the driving input data are subjected to a

data control and interpolation routine, which checks the data for consistency. This data control routine allows SNOWPACK to be run automatically and without large failures using the measured data from more than 80 autonomous and automatic weather and snow stations in the Swiss Alps. SNOWPACK has been in operational use at the IMIS stations for more than 3 years now. The control routines developed could also be useful for data control requirements in other applications.

The statistical model of new snow density and albedo have been derived and evaluated against measurements from high Alpine sites in the Swiss Alps. They are reliable and stable models for those sites but their applicability in other regions and climates need further evaluation.

Based on Monin–Obukhov surface layer similarity theory, we presented a new parameterization of the surface sensible and latent heat fluxes, which accounts for the effect of wind pumping and is also valid for drifting snow conditions. Wind pumping is also included in the near surface thermal properties of the snow. The formulations used are stable and consistent with observations. They are, however, only valid for neutral conditions, which are predominant at our high Alpine sites where the turbulence created mechanically by the topography leads to a near neutral stratification. A successful application of SNOWPACK to larger flat areas, such as the Greenland ice sheet, will benefit from an extension of the model to stable stratification and is in preparation. The current implementation gives, however, already a nice explanation for the different roughness lengths for scalars and momentum over snow surfaces. This new explanation is accomplished without changing the established form of the flux equations.

Also in preparation is a more detailed treatment of the shortwave radiation penetration. At present, a single extinction coefficient is used and penetration is not dependent on wave length. This causes in some cases difficulties in modeling the exact location and thickness of ice lenses. We are also currently working on a model component that describes the interaction of radiation with vegetation in the snow cover for ecological research. This model then also requires a more detailed treatment of radiation transfer.

The profile evaluation shows that the models for microstructure and metamorphism and their links to the thermomechanical properties (Part II) are able to

represent a major part of the structural changes in snow. What is missing at present is a link to the probability of avalanche formation in a certain snow cover. To this end, we will have to extend our description of microstructure to better represent layer interfaces and problematic layers, such as surface hoar. With such an improved description of snow microstructure, a physical model of snow cover instability or a statistical model of avalanche release probability can be formulated. This will be a next step in the SNOWPACK development.

Acknowledgements

We thank Walter Ammann and the Board of the Swiss Federal Institutes of Technology for supporting the work. Many individuals contributed with discussions, knowledge, field experience and with the data sets used in the statistical model developments and evaluations. We especially thank Thomi Stucki, Roli Meister and the Weissfluhjoch Hauswart. The data for the density model was collected by Zenzi Zeidler. We are also very grateful to Matthew Sturm for his prereview. His big effort and comments improved the papers.

Appendix A. Control algorithm for snow depth

The first step in the control algorithm is the elimination of spikes. Spikes are frequent during periods of snowfall. Spikes are detected in the following ways. A possible starting point of a spike in the snow height measurement, hs_i , is marked if the snow depth difference between two consecutive data points exceeds a threshold, T_1 , which depends on the data time resolution:

$$|hs_{i+1} - hs_i| > T_1 \quad (A1)$$

The end of the hypothesized spike, hs_{i+l} , is reached when the snow depth is again close to hs_i , and when the snow depth starts to increase again after it has been decreasing:

$$|hs_{i+l} - hs_i| < T_2 = T_1 t(l)^\beta \text{ and } |hs_{i+l} - hs_i| = \min_{j=1}^{l+1} |hs_{i+j} - hs_i|. \quad (A2)$$

Here $t(l)$ is the time difference of the data points. The exponent, β , is introduced to account for the fact that snow depth differences will never grow linearly in time, i.e. extreme events will only last for a short time. The spike is, however, only eliminated by linear interpolation between hs_i and hs_{i+l} if its height is large relative to its (time) width:

$$\frac{\max_{j=1}^{l-1} |hs_{i+j} - hs_i|}{t(l)} > T_3. \quad (A3)$$

The second step of the control includes in addition to the check for absolute upper and lower bounds and to the elimination of outliers and spikes, a maximum possible increase and decrease in snow height. This differential check requires that missing values are taken into account. If the preceding data point that should be used for comparison is already a missing value, the last valid data point in the time series is used instead. The current snow height measurement, hs_i , is compared to the last valid snow height measurement, hs_{i-l}^{valid} , and is valid if:

$$|hs_i - hs_{i-l}^{\text{valid}}| < T_4 = \begin{cases} \alpha t(l)^\beta, & \text{for decreasing snow depths} \\ \lambda hs_{i-l}^{\text{valid}} t(l)^\beta, & \text{for increasing snow depths.} \end{cases} \quad (A4)$$

It is important to note that for both steps the procedure begins with a valid snow depth reading which is available from the previous model run. Table A1 summarizes the threshold values T_1 through T_4 . At the end of the correction routine, the time series is smoothed using a running average procedure with a variable window width which is currently set at 12 data points.

Table A1
Threshold parameters used for the data control algorithm

T_1	0.06 (m h ⁻¹)
T_2	$\beta = 0.7$
T_3	0.04 (m h ⁻¹)
T_4	$\alpha = 0.13$ (m h ⁻¹), $\beta = 0.7$
T_4	$\gamma = 0.06$, $\beta = 0.7$

Values are for $[hs] = m$ and $[t(l)] = h$.

References

- Albert, M.R., McGilvary, W.R., 1992. Thermal effects due to air flow and vapor transport in dry snow. *J. Glaciol.* 38 (129), 273–281.
- Bartelt, P.B., Lehning, M., this issue. A physical SNOWPACK model for avalanche warning: Part I. Numerical model. *Cold Reg. Sci. Technol.*
- Brutsaert, W., 1975. On a derivable formula for long-wave radiation from clear skies. *J. Water Resour. Res.* 11 (5), 742–744.
- Calanca, P., 2001. A note on the roughness length for temperature over melting snow and ice. *Q. J. R. Meteorol. Soc.* 127, 255–260.
- Colbeck, S.C., 1997. Model of wind pumping for layered snow. *J. Glaciol.* 43 (143), 60–65.
- Durand, Y., Brun, E., Mérindol, L., Guyomarc'h, G., Lesaffre, B., Martin, E., 1993. A meteorological estimation of relevant parameters for snow models. *Ann. Glaciol.* 18, 65–71.
- Fierz, C., Lehning, M., 2001. Assessment of the microstructure-based snow-cover model SNOWPACK: thermal and mechanical properties. *Cold Reg. Sci. Technol.* 33, 123–131.
- Föhn, P.M.B., 2001. Simulation of surface-hoar layers for snow cover models. *Ann. Glaciol.* 32, 19–26.
- Gubler, H., 1998. A model to determine the snow surface properties from remote measurements. *Proc. of Int. Snow Science Workshop (ISSW'98)*. International Snow Science Workshop, Sunriver, Oregon, pp. 35–48.
- Hachikubo, A., Akitaya, E., 1997. Effect of wind on surface hoar growth on snow. *J. Geophys. Res.* 102 (D4), 4367–4373.
- Hampel, F.R., 1985. The breakdown points of the mean combined with some rejection rules. *Technometrics* 27 (2), 95–107.
- Hasager, C.B., Jensen, N.-O., 1999. Surface flux aggregation in heterogeneous terrain. *Q. J. R. Meteorol. Soc.* 125, 2075–2102.
- Högström, U., 1995. Review of some basic characteristics of the atmospheric surface layer. *Bound. Layer Meteorol.* 78, 215–246.
- Kaimal, J.C., Finnigan, J.J., 1994. *Atmospheric Boundary Layer Flows—Their Structure and Measurements*. Oxford Univ. Press, New York, USA, 289 pp.
- Lehning, M., Bartelt, P., Brown, R.L., Russi, T., Stöckli, U., Zimmerli, M., 1999. Snowpack model calculations for avalanche warning based upon a new network of weather and snow stations. *Cold Reg. Sci. Technol.* 30, 145–157.
- Lehning, M., Doorschot, J., Bartelt, P., 2000. A snow drift index based on SNOWPACK model calculations. *Ann. Glaciol.* 31, 382–386.
- Lehning, M., Fierz, C., Lundy, C., 2001. An objective snow profile comparison method and its application to SNOWPACK. *Cold Reg. Sci. Technol.*, 253–261.
- Lehning, M., Bartelt, P.B., Brown, R.L., Fierz, C., Satyawali, P., this issue. A physical SNOWPACK model for the Swiss avalanche warning: Part II. Snow microstructure. *Cold Reg. Sci. Technol.*
- Lundy, C., Brown, R.L., Adams, E.E., Birkeland, K.W., Lehning, M., 2001. A statistical validation of the SNOWPACK model in a Montana climate. *Cold Reg. Sci. Technol.*, 237–247.
- Martin, E., Léjeune, Y., 1998. Turbulent fluxes above the snow surface. *Ann. Glaciol.* 26, 179–183.
- Morris, E.M., 1989. Turbulent transfer over snow and ice. *J. Hydrol.* 105, 205–223.
- Sokratov, S.A., Sato, A., 2000. Wind propagation to snow observed in laboratory. *Ann. Glaciol.* 31, 427–433.
- Sokratov, S.A., Sato, A., 2001. The effect of wind on the snow cover. *Ann. Glaciol.* 32, 116–120.
- Stull, R.B., 1988. *An Introduction to Boundary Layer Meteorology*. Kluwer Academic Publishers, Dordrecht, The Netherlands, 666 pp.